Author version of article published in ACS *Biomacromolecules* 2023 DOI: 10.1021/acs.biomac.3c00662

Transcription-factor-induced aggregation of biomimetic oligonucleotide-*b*-protein micelles

Chloé Grazon,[1,2,3] Elisabeth Garanger,[2] Pierre Lalanne,[2] Emmanuel Ibarboure,[2] James E. Galagan,[4] Mark W. Grinstaff,[3,5*] and Sébastien Lecommandoux[2*]

1 Univ. Bordeaux, CNRS, Bordeaux INP, ISM, UMR 5255, F-33400 Talence, France.

2 Univ. Bordeaux, CNRS, Bordeaux INP, LCPO, UMR 5629, F-33600, Pessac, France.

3 Department of Chemistry, Boston University, Boston, MA 02215, USA.

4 Department of Microbiology, Boston University, Boston, MA 02118, USA.

5 Department of Biomedical Engineering, Boston University, Boston, MA 02215, USA.

ORCID and Emails:

Chloé Grazon 0000-0002-4564-8738	chloe.grazon@u-bordeaux.fr
Elisabeth Garanger 0000-0001-9130-8286	garanger@enscbp.fr
Pierre Lalanne	pierre.lalanne.pro@gmail.com
Emmanuel Ibarboure	Emmanuel.Ibarboure@enscbp.fr
James Galagan 0000-0003-0542-3291	jgalag@bu.edu
Mark W. Grinstaff 0000-0002-5453-3668	mgrin@bu.edu
Sébastien Lecommandoux 0000-0003-0465-8603	sebastien.lecommandoux@u-bordeaux.fr

Abstract

Polymeric micelles, and especially those based on natural diblocks, are of particular interest due to their advantageous properties in terms of molecular recognition, biocompatibility, and biodegradability. We herein report a facile and straightforward synthesis of thermo-responsive elastin-like polypeptide (ELP) and oligonucleotide (ON) diblock bioconjugates, ON-*b*-ELP, through copper-catalyzed azide-alkyne cycloaddition. The resulting thermo-sensitive diblock copolymer self-assembles above its critical micelle temperature (CMT~30°C) to form colloidally stable micelles of ~50 nm diameter. The ON-*b*-ELP micelles hybridize with an ON complementary strand and maintain their size and stability. Next, we describe the capacity of these micelles to bind proteins creating more complex structures using the classic biotin-streptavidin pairing and the specific recognition between a transcription factor protein (TF) and the ON strand. In both instances, the micelles are intact, form larger structures, and retain their sensitivity to temperature.

Keywords: DNA, elastin-like polypeptide, diblock bioconjugates, self-assembly, supramolecular, thermosensitivity

Introduction

Bioinspired and biomimetic materials are a keystone of modern research. Such materials are often constructed from synthetic polymers or one of the three natural biopolymers: oligonucleotides, polypeptides, or polysaccharides. The latter building blocks are useful owing to their advantageous properties such as molecular recognition and binding specificity, biocompatibility, and biodegradability. Within this class of materials, we are particularly interested in self-assembled nanoparticles and micelles,[1–3] which adopt interesting structures, are compositionally complex or stimuli responsive (e.g., heat), and eventually present multivalent presentation of ligands.[4–7] As a first step towards compositionally diverse functional micelles, we are constructing hybrid protein-oligonucleotide-polypeptides systems.

Over the last decade, our group has developed and designed a specific class of biocompatible and biodegradable thermosensitive polymers, namely elastin-like polypeptides (ELPs).[8–12] ELPs are biopolymers derived from the hydrophobic domain of (tropo)elastin and composed of repeating pentapeptide (VPGXG) units.[13] Recombinant production from an artificial gene, in bacteria, provides exquisite precision in terms of sequence and molar mass. ELP sequences exhibit a lower critical solution temperature (LCST) in aqueous solution.[14,15] Fully soluble and hydrated under a cloud point temperature (T_{cp}) at a specific concentration, ELP chains de-solvate and hydrophobically collapse above the T_{cp}.[8,16] Currently, ELPs are widely explored for a variety of applications including protein purification,[17–19] surface coating,[20] tissue engineering,[21–24] drug delivery,[25–29] and more recently for biomimetic purposes for the design of protein vesicles, artificial cells, and membrane-less organelles.[9,30–33] For these different applications, ELPs are combined with other macromolecules such as peptides, proteins, mono-, oligo- or polysaccharides, lipids, natural or synthetic polymers using different synthetic methods *(i.e.*, recombinant technologies, *in vitro* post-translational modifications, or bioconjugation chemistry using natural or non-natural amino residues).

ELP-oligonucleotide (ON) conjugates are rare with limited methodologies available. The first ON-*b*-ELP conjugation was achieved by the teams of Chilkoti and Schmidt.[34] In this work, a 46 bases ON (16.7 kg/mol) was conjugated at the *N*-terminal chain end of a 16.7 kDa ELP (VPGVG). Specifically, the free amine terminal end of the ELP was reacted with an *N*-hydroxysuccinimmide-activated ON immobilized on solid support and, subsequently, cleaved after conjugation. This ELP exhibits a T_{cp} of 35°C-47°C, which depends on the ELP concentration. The

resulting ON-*b*-ELP bioconjugate did not assemble into micelles as the single ON strand was unable to stabilize the structure. However, once hybridized to its complementary sequence, the hyb-ON-*b*-ELP self-assembled into spherical micelles with a critical micelle temperature (CMT) of ~35°C. At 65°C, the hydrodynamic diameter of the micelles was ~39 nm and the radius of gyration ~26 nm (R_g/R_h = 0.7) suggesting that the structures obtained consists of aggregated small micelles.

Recently, the group of Qian and Yang conjugated several commercially available azido-terminated ON sequences (of 21 to 38 bases) to a short commercial hydrophobic ELP with the VPGFG sequence (MW = 476 g/mol) modified at the *C*-terminus by an aliphatic alkyne group.[35,36] A copper(I)-catalyzed azide-alkyne cycloaddition reaction in water/DMSO mixtures afforded the diblock bioconjugates, which were extracted by excision of electrophoresed SDS-PAGE gels. In their first work[35], amphiphilic $(VPGFG)_6$-*b*-ON and $(VPGFG)_6$-*b*-complementaryON bioconjugates (ON from 21 to 38 bases) were hybridized together and formed 55-60 nm diameter vesicles. The vesicles were found sensitive to temperature and shrunk upon an increase in temperature, consistent with other ELP systems[10]. The vesicles encapsulated hydrophobic molecules (nile red, doxorubicin), opening the way for potential drug delivery applications. Building upon this success,[36], they next investigated the influence of the ELP molar mass and the nature of the ON on the $(VPGFG)_y$–*b*-ON_x temperature and morphologies transitions. While $(VPGFG)_6$–*b*-ON_{32} presented a CMT of 25 °C and the $(VPGFG)_5$–*b*-ON_{32} at 33°C, the shorter block $(VPGFG)_4$–*b*-ON_{32} did not show any phase transition, highlighting the importance of a significant hydrophobic block to stabilize the vesicles. Finally, they formed ~210 nm diameter vesicles at 4 °C $(VPGFG)_6$–*b*-ON_{32} which changed morphology above the CMT to adopt a microdroplet shape.

Herein we describe an efficient, facile, and straightforward methodology to chemically conjugate a high molecular weight ELP (42 kg/mol) to a short oligonucleotide (7.5 kg/mol) by copper(I)-catalyzed click chemistry. Surprisingly, none of the above studies used the molecular recognition of DNA in the ON-*b*-ELP as a targeting tool. Inspired by the work of Thayumanavan *et al.*,[37,38,39] and Hamachi *et al.*,[40], where micelles decorated with a small molecular ligand recognize a protein, we investigated whether ON-*b*-ELP micelles bind proteins. ON-*b*-ELP specifically recognizes a protein of interest as demonstrated *via* a classical molecular biotin-streptavidin interaction as well as a transcription factor *via* a sequence dependent DNA binding

event. Importantly, protein binding does not disrupt the micelle and the micelle's thermo-responsiveness functionality remains intact supporting further research into increasingly complex biomimetic materials.

Experimental

Materials

Azidoacetic *N*-hydroxysuccinimidyl ester, propargyl-*N*-hydroxysuccinimidyl ester, copper (II) sulfate pentahydrate, *N*,*N*,*N*,*N*'',*N*''-pentamethyldiethylenetriamine (PMDETA) were purchased from Sigma-Aldrich (FR) along with sinapinic acid and 3-hydroxypicolinic acid for MALDI mass spectrometry analyses. L-sodium ascorbate and *N*,*N*-diisopropylethylamine (DIPEA) were purchased from Alfa Aesar (FR). Amino- and biotin- modified oligonucleotides were purchased from Integrated DNA Technologies (BE) and solubilized in $NaHCO_3$ 0.1 M upon receival (see Table S1 for sequence details). All materials for analysis by electrophoresis were purchased from Biorad (FR) excepted for oligonucleotides length standards from Integrated DNA Technologies (BE). All solvents were purchased from VWR Chemicals (FR). ELP[11,41] and SRTF1[42,43] were produced recombinantly in *E. coli* bacteria following previously reported procedures. Ultrapure water (18 MΩ-cm) was obtained by passing in-house deionized water through a Millipore Milli-Q Biocel A10 purification unit. HEPES buffer saline (HBS) was prepared with 2-[4-(2-hydroxyethyl)piperazin-1-yl]ethanesulfonic acid at 25 mM in water with 150 mM sodium chloride and adjusted to pH 7.4 with NaOH 1M.

Mass spectrometry (MALDI)

Mass spectrometry analyses were performed at the CESAMO (Bordeaux, France) on an AutoflexmaX TOF mass spectrometer (Bruker Daltonics, Bremen, Germany) equipped with a frequency tripled Nd:YAG laser emitting at 355 nm. Spectra were recorded in the positive-ion mode and with an accelerating voltage of 19 kV. Different matrices and protocols were used depending on the nature of the sample. No calibration was performed. The starting ELP and ON served as reference for N_3-ELP and ON-alk, respectively. The deposits and analyses were done in duplicate.

Freeze-dried ELP and N_3-ELP were dissolved in a mixture of water and acetonitrile (1:1) at 10 mg/mL. Sinapinic acid matrix was prepared as a supersaturated solution (ca.10 mg/mL) in a

mixture of water/acetonitrile/trifluoroacetic acid (49.9:50:0.1). The solutions were combined in a 20:2 or 18:2 volume ratio of matrix to sample. 1.5 to 2 µL of the resulting solution were deposited onto the sample target and vacuum-dried.

ON and ON-alk were prepared at 10 mg/mL in H_2O. In parallel a matrix of 3-hydroxypicolinic acid (3-HPA, 50 mg/mL in acetonitrile/ H_2O (1:1)) was prepared. The sample was deposited on the analysis plate using the sandwich method: a matrix droplet was dried, followed by a droplet of oligonucleotide dried and then finally covered by another droplet of 3-HPA matrix.

ON-*b*-ELP at 0.17 mg/mL in HBS+0.1% TFA was concentrated and desalted on a C_{18} Ziptip and eluted with 2µL of acetonitrile/ H_2O (1:1). In parallel a matrix of 3-hydroxypicolinic acid (3-HPA, 50 mg/mL in acetonitrile/ H_2O (1:1)) was prepared. The sample was deposited on the analysis plate using the sandwich method: a matrix droplet was dried, followed by a droplet of ON-*b*-ELP dried and then finally covered by another droplet of 3-HPA matrix.

Gel electrophoresis

Gel electrophoresis analyses were carried on SDS-PAGE gels (BioRad MiniPROTEAN TGX, stain-free, 4%-20% gradient), on purified and un-purified samples. Around 2.5 µg of each sample were loaded on the gel in 10 µL of ultrapure water/Laemli (1/1). Electrophoresis was run using a Tris/Glycine/SDS buffer (Biorad), with a BioRad MiniPROTEAN® Tetra System device (25 mA, 45 min). The gel was imaged with a BioRad GelDocTM EZ Imager.

Absorption measurements

Absorption measurements were performed on a UV5 Nano Mettler (Path = 0.1 mm or 1 mm) on 3 µL samples at room temperature in order to determine ON or ON-*b*-ELP concentrations, using ε_{ON}@260nm= 221,100 $M^{-1}cm^{-1}$.

Dynamic light scattering (DLS)

DLS experiments were carried out on a Horiba SZ-100 nanoPartica with a laser source at λ = 532 nm and at a scattering angle of 90° and constant position in the cuvette (constant scattering volume). 15 µL samples were analyzed in quartz cuvette of 1.5 mm path. Three independent measurements of 3 runs of 10 sec were recorded. Temperature ramps were adjusted for each type of sample. For all the ramps, the temperature step was 2 °C and a 120 second-stabilization time

was applied between each temperature. The Count Rate (CR) was defined as the mean scattered intensity. This scattered intensity was plotted against temperature and the T_{cp} of the ELP, as well as the CMT of the diblocks, was defined at the point where the CR starts increasing. Hydrodynamic diameters (also called Z-average sizes - D_z) were calculated using the cumulant method based on the scattered intensity from the particles.

Confocal microscopy

Scanning confocal microscopy images were acquired on an inverted Leica TCS SP5 microscope equipped with an HCX PL APO 63X, NA 1.4 oil immersion objective in fluorescence mode. The laser outputs were controlled via the Acousto-Optical Tunable Filter (AOTF) and the collection window using the Acousto-Optical Beam Splitter (AOBS) and photomultiplicators (PMT) as follows: Nile Red was excited with a laser at 561 nm (12.5%) and measured with emission settings at 570-600 nm. The Helium-Neon laser at 633 nm (10%) was only used in transmission mode. Images were collected in simultaneous mode using a rate at 400 Hz and a resolution of 512×512 pixels.

In a typical experiment, 100 µL of sample at 0.17 mg/mL in HBS were prepared and 1 µL of Nile Red at 0.2 mg/mL in acetonitrile were added. 10 µL of the labelled solutions were injected in a homemade chamber (previously saturated with BSA at 10 mg/mL and intensively washed to prevent nonspecific adsorption of the particles on the glass slide). The samples were heated/cooled using a precise Peltier temperature-controlled microscope stage (Linkam, PE100) equipped with a Linkam PE95 digital temperature control unit. A rate of 5°C.min^{-1} for increasing and decreasing temperature was applied to all samples. To this chamber, 1 µL of the protein of interest (SA or BSA or SRTF1) was added above the CMT (at 40°C).

Transmission Electron Microscopy (TEM).

ON-*b*-ELP micelles (0.17 mg/mL in HBS) warmed at 37°C were deposited on formvar-coated copper grids in an oven at 37°C. After removal of the sample drop and air drying of the grid, uranyl acetate (3wt%) was deposited at room temperature onto the grids to contrast the objects. After removal of the contrasting agent drop and air drying of the grid, the objects were imaged on a Hitachi H7650 electron microscope (80 kV) located in the Bordeaux Imaging Center, France.

Synthesis of N_3-ELP.

To a solution of ELP[M_1V_3-100] (32 mg, 0.76 µmol) in DMF (2.7 mL) was added *N*,*N*-diisopropylethylamine (1.05 µL, 6.1 µmol) and a solution of azidoacetic *N*-hydroxysuccinimide ester (0.75 mg, 3.81 µmol) in DMF (0.5 mL). The mixture was degassed with nitrogen then stirred for 2 days at room temperature. The solution was diluted with water (4 mL) then dialyzed for 2 days against pure water in dialysis tubing (MWCO 10 kDa) (changing water 3 times per day, the two first baths at room temperature and the following at 4°C). The final product was obtained by lyophilization (white powder, 31.2 mg, 95% yield). N_3-ELP was characterized by MALDI mass spectrometry using the starting ELP as reference.

Theoretical ELP[M_1V_3-100] molar mass: 42,085 g/mol; Experimental m/z= 42,096 g/mol (z=1)

Theoretical N_3-ELP[M_1V_3-100] molar mass: 42,168 g/mol; Experimental m/z= 42,186 g/mol (z=1)

Synthesis of ON-alk.

To a solution of ON (1 mM, 10 mg, 1.3 µmol) in $NaHCO_3$ at 0.1 mol.L^{-1} (1.3 mL) was added a solution of propargyl-*N*-hydroxysuccinimidyl ester (7.5 mg, 33 µmol) in DMSO (1.3 mL). The reaction mixture was stirred overnight at room temperature, then diluted with water (~5 mL) and dialyzed for 2 days against ultrapure water in dialysis tubing (MWCO 1 kDa) (changing water 3 times per day, the two first baths at room temperature and the following at 4°C). The purified ON-alk solution was concentrated by freeze-drying and the obtained white powder was recovered in ultrapure water at 500 µM in 75% yield. ON-alk was characterized by MALDI mass spectrometry using the starting ON as reference.

Theoretical ON molar mass: 7,504 g/mol; Experimental m/z= 7,597.3 g/mol (z=1)

Theoretical ON-alk molar mass: 7,614 g/mol; Experimental m/z= 7,785.4 g/mol (z=1)

Synthesis of the ON-*b*-ELP bioconjugate.

To a solution of N_3-ELP (20 mg, 0.5 µmol) in DMF (1 mL) were added a solution of ON-alk (2.4 mg, 0.3 µmol) in water (480 µL), 200 µL of triethylammonium acetate buffer at 2 mol/L and a solution of sodium ascorbate (2.9 µmol) in water (5 µL). The reaction mixture was degassed with N_2 for 10 min then a solution of copper sulfate pentahydrate (1 µmol) and PMDETA (1 µmol) in water (5 µL) was added. A second degassing was performed with N_2 for 10 min and the mixture was then stirred for 120 hrs at room temperature. At the end of the reaction, around 50% of the

ELP had reacted and was conjugated to the ON, implying a 75% reaction efficiency. The solution was next diluted with water (2 mL) and copper-sequestrant beads (Cuprisorb®) were added to the mixture, and dialyzed for 2 days against pure water (to remove small molecules and solvents from the reaction as well as the unreacted ON) in dialysis tubing (MWCO 25 kDa) (changing water 3 times per day, 4°C). The solution of the bioconjugate was transferred to a 1.5 mL centrifugal tube and concentrated by ultracentrifugation (3 kDa, 30 min, 3800 rpm, 5°C) and. The retentate was subjected to a hot spin (1 min, 12,000 rpm, 30°C) to remove the unreacted N_3-ELP (recovered in the pellet) from the ON-*b*-ELP bioconjugate (recovered in supernatant). The final concentration of the ON-*b*-ELP diblock was estimated by absorbance (taking ε_{ON}@260nm= 221,100 $M^{-1}cm^{-1}$). Around 4 mL of the ON-*b*-ELP at 35 µM (1.7 mg/mL, 7.0 mg) were obtained with a 50% molar yield.

Theoretical ON molar mass: 49,782 g/mol; Experimental m/z ~ 50,3 g/mol (z=1).

Results and discussion

Synthesis of the amphiphilic diblock ON-b-ELP bioconjugate

We recombinantly produced the temperature-responsive ELP[M_1V_3-100], with the primary sequence MW-[(VPGVG)(VPGMG)$(VPGVG)_2]_{25}$ and of 42 kDa molar mass, *in Escherichia coli* (*E. coli*) bacteria following previously reported procedures.[41] We selected this 100 repeat unit-ELP (ELP[M_1V_3-100], simply designated as ELP going forward) because of its thermo-responsive properties, namely the range and minimal dependence of its cloud point temperature (T_{cp}) versus molar concentration,[41] and the range of critical micelle temperature (CMT) when conjugated to a hydrophilic block.[10] This ELP displays a sub-ambient lower critical solution temperature (LCST)[41], and a cloud point temperature (T_{cp}) of 25 °C at a concentration of 3.2 µM in HEPES buffer saline pH 7.4 (HBS).

Next, we identified the oligonucleotide (ON) sequence as bioconjugate's hydrophilic segment to ensure high water solubility and protein molecular recognition. More precisely, the ON sequence (24 bases, 7.5 kDa, Table S1) comprises a 20 base-cognate binding region to a known transcription factor (TF) protein,[42,43] and is equipped with four additional thymine nucleotides at the 5' extremity to act as spacer with the ELP block and reduce steric hindrance between the ON-

b-ELP micelles and the TF. We purchased this ON with an hexylamine linker at the 5' extremity for subsequent coupling to the ELP.

We performed the Cu(I)-catalyzed azide-alkyne Meldal[44]/Sharpless[45] cycloaddition (CuAAC) reaction to prepare the diblock ON-*b*-ELP bioconjugate in water. To accomplish this, we installed an azido group at the *N*-terminal chain end of the ELP *via* an amidation reaction using azidoacetic *N*-hydroxysuccinimide ester in DMF (Figure 1A). In parallel, we introduced an aliphatic alkyne group at the 5'amino-ON by an amidation reaction using propargyl-*N*-hydroxysuccinimidyl ester in a DMSO/$NaHCO_3$ 0.1 M (1:1) mixture (Figure 1B). MALDI-TOF mass spectrometry confirmed the functionalization of each block (Figure 1C).

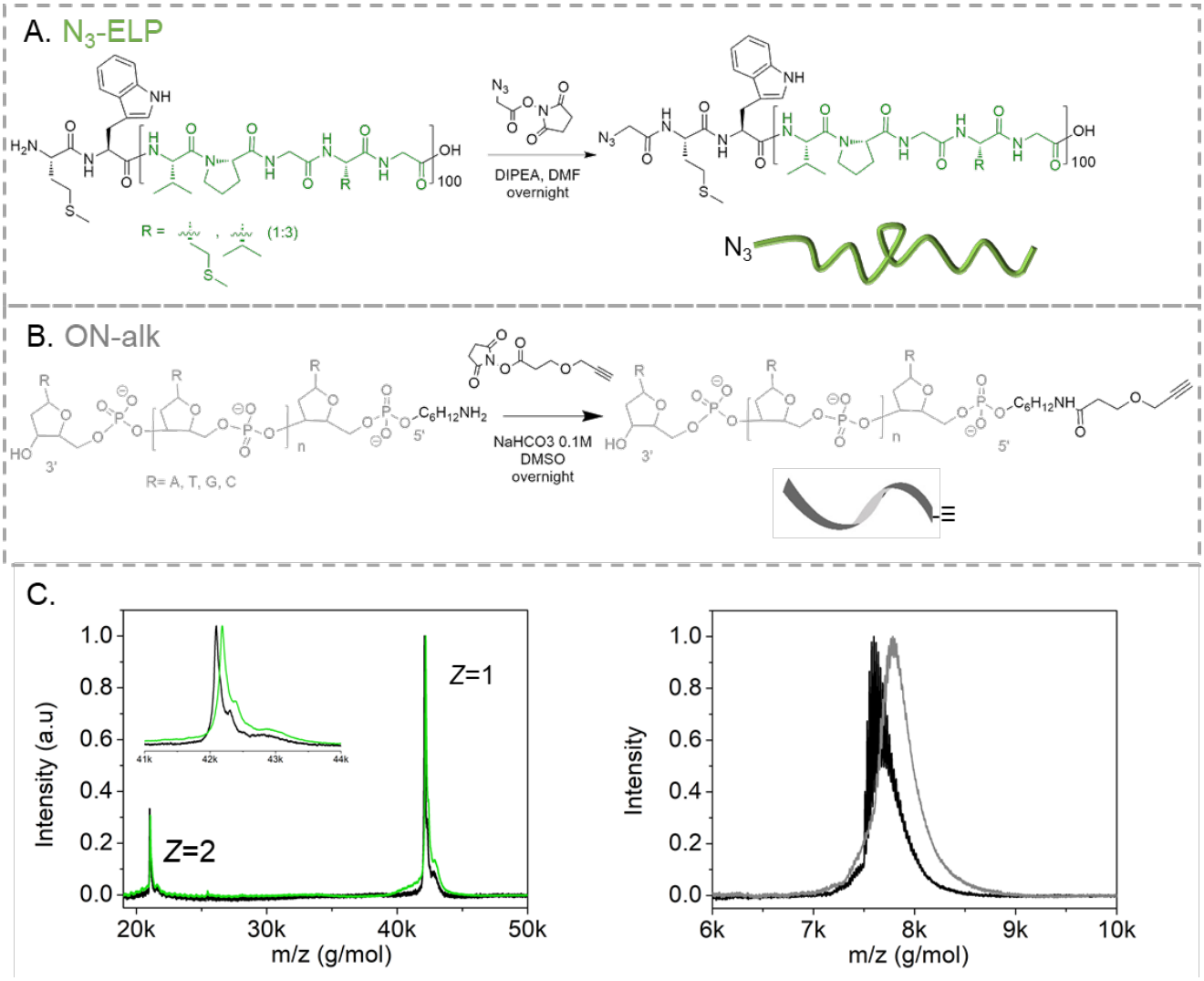

Figure 1. A. Synthetic scheme to access the azido-terminated ELP (N_3-ELP). B. Synthetic scheme to access the alkyne functionalized ON (ON-alk). C. MALDI-TOF mass spectra of both biopolymers. Left: N_3-ELP (green, m/z = 42,186

g/mol for z=1 and 21,075 g/mol for z=2) and initial ELP (black). Right: ON-alk (grey, m/z=7,785 g/mol) and initial ON (black).

Finally, we synthesized the ON-*b*-ELP bioconjugate using the CuAAC reaction under inert atmosphere (in order to avoid ELP oxidation in particular at methionine residues) in a mixture of water and DMF (1:2) and with a 1.7-fold excess of N_3-ELP (Figure 2A). We monitored the reaction by gel electrophoresis (SDS-PAGE) analysis, and by day 4 the reaction had stopped progressing with approximately 50% of the N_3-ELP reacted. We then added copper-sequestrants beads to the reaction mixture and dialyzed the filtrate at 4 °C against ultrapure water using 25 kDa dialysis tubing to remove the unreacted ON-alk and other chemical reactants. The solution was then concentrated with a centrifugal filter unit and subjected to a hot spin (30°C) to separate the unreacted N_3-ELP (aggregated in the pellet) from the ON-*b*-ELP bioconjugate (dispersed in the supernatant). We confirmed success of the reaction and purification procedure by MALDI-TOF and SDS-PAGE analysis as illustrated in Figures 2B and S1.

Noteworthy, the click reaction used here involves an ELP functionalized at the *N*-terminus with an azido group, while our team previously used alkyne-terminated ELPs for coupling to azido-functionalized hydrophilic blocks.[11,12] The coupling efficiency herein is similar to the alternative coupling procedure previously explored (80-90%), highlighting the versatility of the CuAAc reaction in the synthesis of amphiphilic diblock bioconjugates. Although we see excellent utility in this CuAAc reaction, we recognize the significant advancements in Cu-free click chemistry[46,47] and this is another synthetic approach one should consider in preparing such ON conjugates.

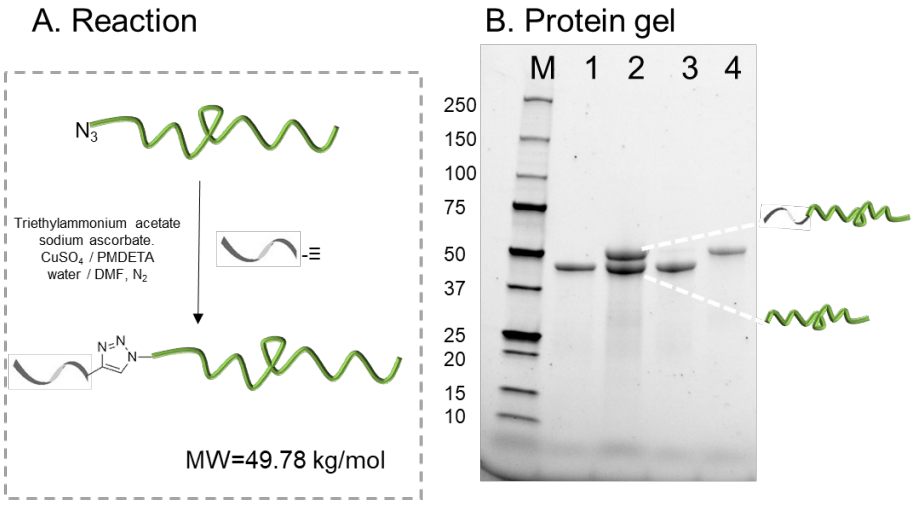

Figure 2. A. Synthetic scheme of the ON-*b*-ELP bioconjugate. B. Stain-free SDS-PAGE (4-12% gradient) gel. M: Protein size marker (kDa); Line 1: N_3-ELP; Line 2: reaction mixture after dialysis; Line 3: Pellet after the hot spin (unreacted excess N_3-ELP); Line 4: Supernatant after the hot spin (purified ON-*b*-ELP bioconjugate).

Temperature-triggered self-assembly of the ON-b-ELP bioconjugate and micelle hybridization with a complementary ON strand

We monitored the temperature response of the ON-*b*-ELP by dynamic light scattering (DLS) in HBS. We first investigated the influence of the bioconjugate concentration on the CMT (Figures S2 and S3). From 0.02 mg/mL (0.4 µM) to 0.77 mg/mL (15 µM), all the amphiphilic ON-*b*-ELP diblocks are temperature-responsive, with CMT ranging between 28 and 30°C. These higher CMTs as compared to the T_{cp} of the starting ELP are consistent with the conjugation of a highly hydrophilic ON block to the ELP.[11,12] At all concentrations, nanoparticles formed above the CMT are highly monodisperse with a Z-averaged hydrodynamic diameter (D_z) of 46±2 nm at 37±1 °C (n=6 for each set of measurements, size dispersity < 0.1) (Figure S3). For the remainder of this study, we performed experiments at 0.17 mg/mL (3.4 µM, Figures S2, S3, S4) of ON-*b*-ELP bioconjugate to ensure quality DLS data, in particular the scattered light intensity, and to use minimal amount of materials. At 3.4 µM, the CMT of the bioconjugate is around 30°C. The transition between soluble ON-*b*-ELP chains in HBS buffer below the CMT, to nanoparticles above the CMT, is reversible with very low hysteresis (Figures S2, S3) and occurs over a larger temperature range (between 30 °C and 45 °C) (Figures S2, S3 and Figure 3B). For comparison, the ELP alone, at similar molar concentrations, displays a sharp temperature transition (between 25 °C and 30 °C) with a CMT of 25 °C and forms reversible disperse coacervates of 100-1000 nm

(Figures 3B and S5). These data are consistent with previous studies performed on micellar structures of polysaccharide-*b*-ELPs, where the introduction of the hydrophilic block stabilizes the coacervates formed by the ELPs.[11,12] Consequently, ON-*b*-ELP bioconjugates likely self-assemble above the CMT into spherical micellar nanoparticles with the ELP aggregated in the core and the hydrophilic ON displayed on the outer shell insuring the colloidal stability of the resulting nanoparticles. We confirmed the formation of these micelles by Transmission Electron Microscopy (Figure S6) using uranyl acetate as a contrast agent. The spherical nanoparticles with a dry core diameter are around 35 nm in diameter. In addition, we performed confocal microscopy imaging (Figure S7). Specifically, we labelled the ON-*b*-ELP micelles with the lipophilic Nile Red dye and deposited them on a glass slide. Above the CMT, ON-*b*-ELP micelles clearly appear as small red dots (Figure S7 right image), while below the CMT, ON-*b*-ELP bioconjugates are barely visible and only a diffuse red fluorescence background is detected (Figure S7 left image).

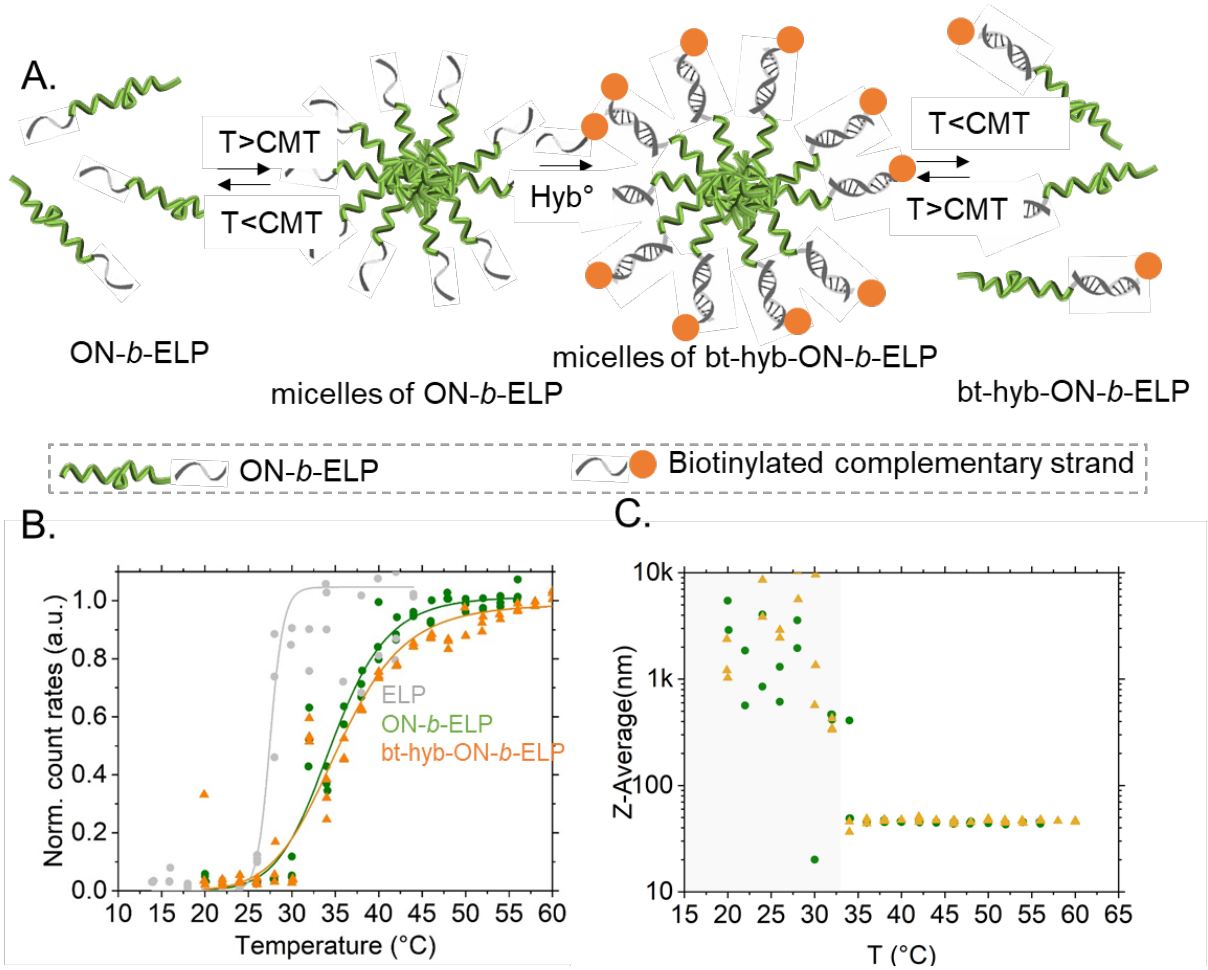

Figure 3. A. Representative scheme of the ON-*b*-ELP self-assembly into micelles above the CMT and hybridization with a complementary biotinylated ON strand (bt-hyb-ON-*b*-ELP). B. Normalized scattering intensity (count rates) and C. Z-averaged hydrodynamic diameter measured of the diblocks at 3.4 µM by DLS at different temperatures in HBS. Each measurement was performed three times and all the raw data are plotted.

Next, we hybridized the micelles of ON-*b*-ELP at 0.17 mg/mL in HBS with a complementary ON sequence tagged with a biotin group at the 5' extremity (Table S1). We mixed the ON-*b*-ELP at room temperature with one molar equivalent of the ON complementary (regarding the ON-*b*-ELP chains), followed by increasing the temperature to 60 °C for 15min (*i.e.,* above the CMT=30 °C of the ON-*b*-ELP and the T_m=56 °C of the ON), and then slowly cooled the sample to room temperature. Note that at 37 °C, we are 20 °C below the T_m of the ON, ensuring that ON is hybridized with its complementary strand. Hybridization affords the bt-hyb-ON-*b*-ELP micelles with a hydrodynamic diameter of 46±2nm at 37±1 °C (n=6) (Figures 3B and 3C, S8).

Specific biorecognition and aggregation of bt-hyb-ON-b-ELP micelles with streptavidin

Given the well-established streptavidin-biotin affinity, we next evaluated the biorecognition of bt-hyb-ON-*b*-ELP micelles to streptavidin (SA, 53 kDa, isoelectric point – pI~5) (Figure S9). We added SA at a final concentration of 4 μM (1.25 mol equiv. to biotin) to a dispersion of bt-hyb-ON-*b*-ELP micelles (0.17 mg/mL, 3.4 μM) in HBS at 37°C. In less than 10 min, we observed a strong increase of the scattered light intensity and a gradual increase of hydrodynamic diameters of particles in the dispersion (Figure S9B). Autocorrelation curves of the micelle dispersions also shift to longer delay times in the presence of SA, consistent with an increase in size, while remaining unchanged in the presence of bovine serum albumin (BSA, 66 kDa, pI ~ 4.7) used as control (Figure S9C). All these observations support the formation of bt-hyb-ON-*b*-ELP micelle aggregates in the presence of SA. We then applied a cooling and a heating temperature ramp to these aggregates and performed DLS. Although the hydrodynamic diameter indicates the presence of micrometer-sized objects (Figure S9D), the scattered light intensity still shows a clear shift around 30 °C (Figure S9E) with a ~10 fold increase in intensity. This result is consistent with increased contraction of the ELP cores due to their dehydration,[8] which suggests that the SA-aggregated bt-hyb-ON-*b*-ELP micelles still respond to temperature.

As before, we also confirmed the formation of these aggregates by confocal microscopy imaging (Figure S10). We labeled bt-hyb-ON-*b*-ELP micelles with the lipophilic Nile Red dye and deposited on a glass slide. In the presence of SA, micrometric aggregates are clearly visible, (Figure S10B right image) while bt-hyb-ON-*b*-ELP micelles alone (3.4 μM) appear as small individual red dots (Figure S10B left image).

Transcription factor-induced aggregation of hyb-ON-b-ELP micelles

We then investigated the specific recognition of these biomimetic micelles to a protein. We are particularly interested if the presence of the protein will destabilize the micelles by shifting the hydrophilic-lipophilic balance. Moreover, there are very few examples of colloids recognizing proteins, and, those that do, rely on a small molecule-protein affinity (as the well-known biotin-streptavidin). Indeed, beyond the simple molecular recognition of biotin and streptavidin, the hyb-ON-*b*-ELP micelles possess a DNA encoding sequence, which enables sequence-specific recognition of a transcription factor (TF). TFs play an important role in biology as gene-regulating proteins and are in fact an example of a natural hybrid oligonucleotide-protein system. We selected

the TF SRTF1 (22 kDa, pI ~5.4), which mediates the ketosteroid-dehydrogenase gene and specifically binds to a 20 bp palindromic sequence.[42]

For these experiments, we hybridized the ON-*b*-ELP micelles with a non-biotinylated complementary strand (Table S1) to obtain hyb-ON-*b*-ELP. The absence of biotin at the 5' terminus of the complementary strand does not significantly change the behavior of the micelles (Figure 4). The hyb-ON-*b*-ELP bioconjugate exhibits a CMT of around 30 °C in HBS at 3.4μM and forms, above the CMT, micelles with a hydrodynamic diameter of 49±2 nm at 37±1°C (Figure S11). Interestingly, at 37°C, micelles of bt-hyb-ON-*b*-ELP and hyb-ON-*b*-ELP possess a slightly larger hydrodynamic diameter than ON-*b*-ELP, 46±2nm and 49±2 nm respectively, while the CMT remains at ~30°C (Figure 3C). The hydrodynamic diameter is slightly smaller for biotin (bt) version of the ON and unexpected. One possible explanation may be that the bt confers more hydrophocity to the structure and results in a more collapsed structure. Future studies will look into this change and what other ODN modifications give such a result. To the hyb-ON-*b*-ELP micelles at 3.4 μM and 37±1 °C, we sequentially added SRTF1. At 0.12 μM SRTF1, no significant change occurs, the autocorrelation function is still neat and the hydrodynamic diameter of the micelles is around 50±2 nm. At 1.2 μM SRTF1, *i.e.* ~0.4 molar equiv. with respect to the ON, there is still no change in the autocorrelation function. However, upon closer observation of the data, the scattered light intensity increases from around 1,500 kCPs to 2,500 kCPs; a hallmark of the formation of larger objects. In agreement with the increase of the scattering intensity, the hydrodynamic diameter of the micelles also slightly increases to 58±3nm. Finally, upon addition of 12 μM SRTF1, the autocorrelation curve shifts toward longer delay times. This change is accompanied with a 3.5-fold increase in the scattered intensity (count rates) and aggregates of 720±170 nm in size. Similarly to our previous observations with the [SA(bt-hyb-ON-*b*-ELP)] aggregates, hyb-ON-*b*-ELP micelles decorated with SRTF1 are still thermally-responsive (Figure 4 C-D). More importantly, despite the presence of the hydrophilic SRTF1 protein bound to the hyb-ON-*b*-ELP, the bioconjugate maintains similar temperature-responsiveness. DLS control experiments (Figure S12) performed on SRTF1 alone, SRTF1+ON, or HBS do not show any change with temperature, confirming the role of the ELP in this transition.

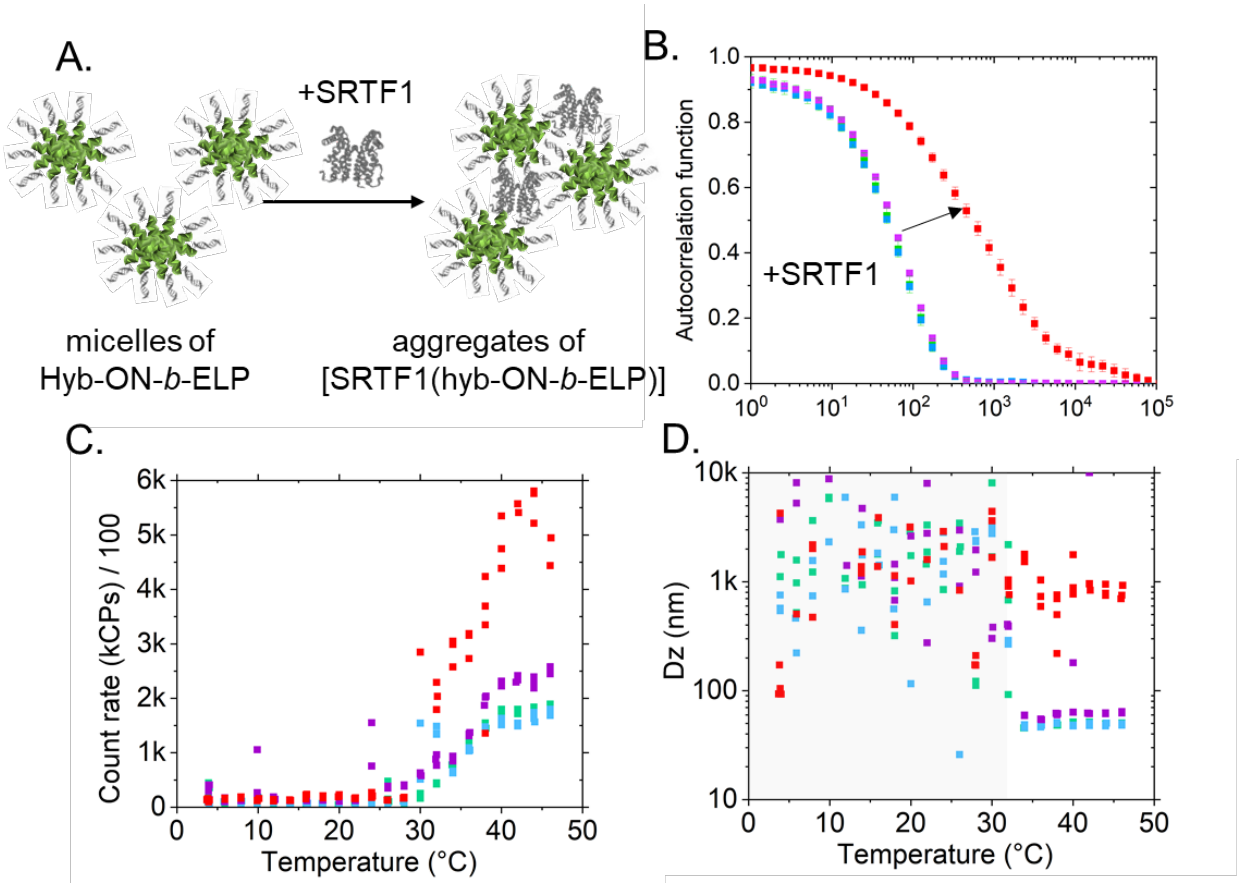

Figure 4. A Representative scheme of the hyb-ON-*b*-ELP self-assembly into micelles above the CMT and aggregation upon SRTF1 addition. To a dispersion of hyb-ON-*b*-ELP micelles at 3.4 µM (0.17 mg/mL – green points) in HBS, sequential additions of SRTF1 (up to 0.12 µM - blue, 1.2 µM-purple, and 12 µM-red points) were performed. B. Autocorrelation functions at 37±1 °C (standard deviation error bar on n=3). C. Scattered light intensity (count rates) and D. Z-averaged hydrodynamic diameters of hyb-ON-*b*-ELP micelles with increased concentrations of SRTF1 as measured by DLS at different temperatures in HBS. For each temperature, the n=3 points are represented on graphs C and D.

Finally, we confirmed aggregates formation using confocal microscopy. We labeled micelles of hyb-ON-*b*-ELP at 3.4 µM at 40 °C with Nile Red and then added SRTF1 at 12 µM (Figure 5 left panel). As with the SA system, we observed micrometric aggregates appearing, once again confirming the specific recognition of the micelles to the target transcription factor.

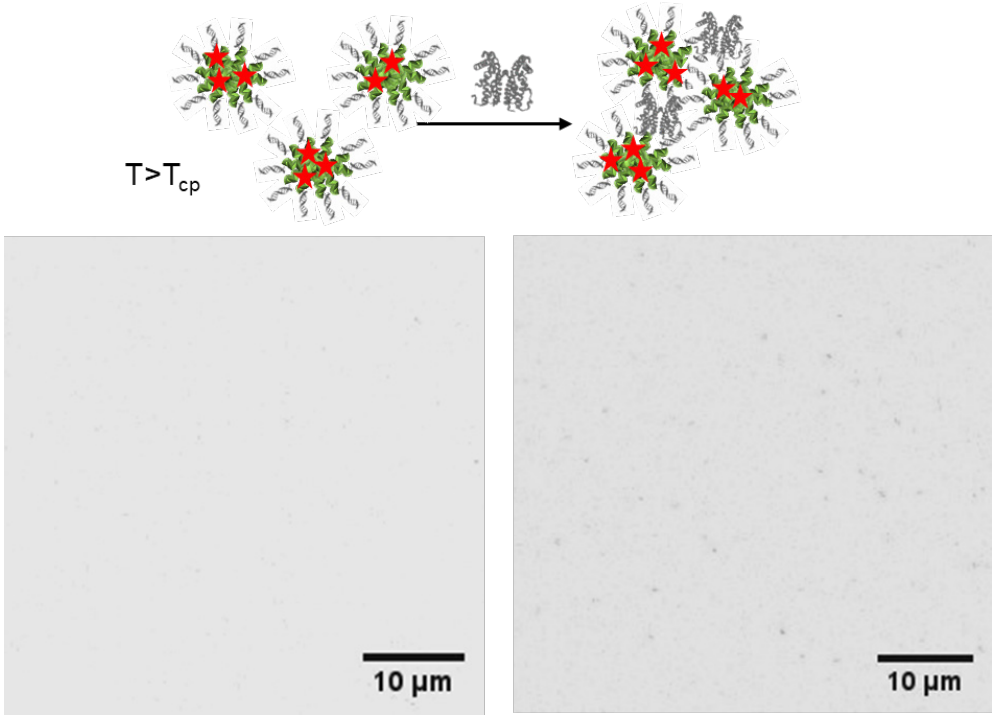

Figure 5. Confocal microscopy images of hyb-ON-*b*-ELP (3.4 µM) stained with Nile Red in HBS at 40 °C (left) and upon addition of SRTF1 (12 µM - right). Inverted colors image.

Conclusions

We describe the successful synthesis and purification of hybrid oligonucleotide-*b*-elastin-like polypeptide (ON-*b*-ELP) diblock bioconjugates. These conjugates self-assemble into 46±2 nm sized micellar structures at 37 °C in HEPES buffer saline. Upon hybridization with a complementary ON strand, the ON-*b*-ELP bioconjugate and micelles retain their thermal properties and hydrodynamic diameters. The ON component of the ON-*b*-ELP bioconjugate and micelles provides a handle for additional supramolecular formation *via* complexation with a protein using either a classical biotin-streptavidin interaction or the transcription factor SRTF1. The micelles remain intact after protein binding in contrast to previous reports,[37–40] where the presence of the protein destabilizes the micelles. Further, despite the high molar mass of the [protein(hyb-ON-*b*-ELP)] assemblies, the ELPs are temperature responsive with a T_{cp} around 30°C. These two later findings provide a strategy to synthesize increasing complex functional micelles using oligonucleotides, polypeptides, and proteins. While intense research efforts are ongoing to study oligonucleotides-peptides coacervates,[48] or polyelectrolytes complex micelles,[49] there are few examples of such purely bio-based soft aggregates induced by a specific bio-recognition. Such

biomimetic micelle recognition is likely of interest for the fabrication of larger supramolecular assemblies as well as for potential biomedical applications such as protein capture for sensing.

Supporting Information

Oligonucleotides sequences, complementary MADI-TOF, dynamic light scattering, transmission electron microscopy and confocal microscopy measurements on ELP, ON-b-ELP, hybON-b-ELP with/without protein addition are available in the supporting information.

Acknowledgements

CG acknowledges Marie-Skłodowska-Curie Fellowship from the European Union under the program H2020 (Grant 749973). PL acknowledges the ENS Paris-Saclay for his master internship grant. The authors also acknowledge Karthika Sankar and Pauline Coutand for technical support on this project. Continuous support from Univ. Bordeaux, CNRS and Bordeaux INP is greatly acknowledged.

References

(1) Min, Z.; Xu, B.; Li, W.; Zhang, A. Combination of DNA with Polymers. *Polym. Chem.* **2021**, *12* (13), 1898–1917. https://doi.org/10.1039/D0PY01777A.

(2) Sun, H.; Yang, L.; Thompson, M. P.; Schara, S.; Cao, W.; Choi, W.; Hu, Z.; Zang, N.; Tan, W.; Gianneschi, N. C. Recent Advances in Amphiphilic Polymer–Oligonucleotide Nanomaterials via Living/Controlled Polymerization Technologies. *Bioconjug. Chem.* **2019**, *30* (7), 1889–1904. https://doi.org/10.1021/acs.bioconjchem.9b00166.

(3) Whitfield, C. J.; Zhang, M.; Winterwerber, P.; Wu, Y.; Ng, D. Y. W.; Weil, T. Functional DNA–Polymer Conjugates. *Chem. Rev.* **2021**, *121* (18), 11030–11084. https://doi.org/10.1021/acs.chemrev.0c01074.

(4) Duan, H.; Donovan, M.; Hernandez, F.; Di Primo, C.; Garanger, E.; Schultze, X.; Lecommandoux, S. Hyaluronic-Acid-Presenting Self-Assembled Nanoparticles Transform a Hyaluronidase HYAL1 Substrate into an Efficient and Selective Inhibitor. *Angew. Chem. Int. Ed.* **2020**, *59* (32), 13591–13596. https://doi.org/10.1002/anie.202005212.

(5) Liu, M.; Apriceno, A.; Sipin, M.; Scarpa, E.; Rodriguez-Arco, L.; Poma, A.; Marchello, G.; Battaglia, G.; Angioletti-Uberti, S. Combinatorial Entropy Behaviour Leads to Range Selective Binding in Ligand-Receptor Interactions. *Nat. Commun.* **2020**, *11* (1), 4836. https://doi.org/10.1038/s41467-020-18603-5.

(6) Duan, H.; Donovan, M.; Foucher, A.; Schultze, X.; Lecommandoux, S. Multivalent and Multifunctional Polysaccharide-Based Particles for Controlled Receptor Recognition. *Sci. Rep.* **2018**, *8*, 14730. https://doi.org/10.1038/s41598-018-32994-y.

(7) Bonduelle, C.; Oliveira, H.; Gauche, C.; Huang, J.; Heise, A.; Lecommandoux, S. Multivalent Effect of Glycopolypeptide Based Nanoparticles for Galectin Binding. *Chem. Commun.* **2016**, *52* (75), 11251–11254. https://doi.org/10.1039/C6CC06437J.

(8) Garanger, E.; MacEwan, S. R.; Sandre, O.; Brûlet, A.; Bataille, L.; Chilkoti, A.; Lecommandoux, S. Structural Evolution of a Stimulus-Responsive Diblock Polypeptide Micelle by Temperature Tunable Compaction of Its Core. *Macromolecules* **2015**, *48* (18), 6617–6627. https://doi.org/10.1021/acs.macromol.5b01371.

(9) Zhao, H.; Ibarboure, E.; Ibrahimova, V.; Xiao, Y.; Garanger, E.; Lecommandoux, S. Spatiotemporal Dynamic Assembly/Disassembly of Organelle-Mimics Based on Intrinsically Disordered Protein-Polymer Conjugates. *Adv. Sci.* **2021**, *8* (24), 2102508. https://doi.org/10.1002/advs.202102508.
(10) Zhao, H.; Ibrahimova, V.; Garanger, E.; Lecommandoux, S. Dynamic Spatial Formation and Distribution of Intrinsically Disordered Protein Droplets in Macromolecularly Crowded Protocells. *Angew. Chem. Int. Ed.* **2020**, *59* (27), 11028–11036. https://doi.org/10.1002/anie.202001868.
(11) Levêque, M.; Xiao, Y.; Durand, L.; Massé, L.; Garanger, E.; Lecommandoux, S. Aqueous Synthesis and Self-Assembly of Bioactive and Thermo-Responsive HA- *b* -ELP Bioconjugates. *Biomater. Sci.* **2022**, *10*, 6365–6376. https://doi.org/10.1039/D2BM01149B.
(12) Xiao, Y.; Chinoy, Z. S.; Pecastaings, G.; Bathany, K.; Garanger, E.; Lecommandoux, S. Design of Polysaccharide- *b* -Elastin-Like Polypeptide Bioconjugates and Their Thermoresponsive Self-Assembly. *Biomacromolecules* **2020**, *21* (1), 114–125. https://doi.org/10.1021/acs.biomac.9b01058.
(13) Meyer, D. E.; Chilkoti, A. Genetically Encoded Synthesis of Protein-Based Polymers with Precisely Specified Molecular Weight and Sequence by Recursive Directional Ligation: Examples from the Elastin-like Polypeptide System. *Biomacromolecules* **2002**, *3* (2), 357–367. https://doi.org/10.1021/bm015630n.
(14) Urry, D. W.; Long, M. M.; Cox, B. A.; Ohnishi, T.; Mitchell, L. W.; Jacobs, M. The Synthetic Polypentapeptide of Elastin Coacervates and Forms Filamentous Aggregates. *Biochim. Biophys. Acta BBA - Protein Struct.* **1974**, *371* (2), 597–602. https://doi.org/10.1016/0005-2795(74)90057-9.
(15) Lee, J.; MacOsko, C. W.; Urry, D. W. Phase Transition and Elasticity of Protein-Based Hydrogels. *J. Biomater. Sci. Polym. Ed.* **2001**, *12* (2), 229–242. https://doi.org/10.1163/156856201750180942.
(16) Meyer, D. E.; Chilkoti, A. Quantification of the Effects of Chain Length and Concentration on the Thermal Behavior of Elastin-like Polypeptides. *Biomacromolecules* **2004**, *5* (3), 846–851. https://doi.org/10.1021/bm034215n.
(17) Yeboah, A.; Cohen, R. I.; Rabolli, C.; Yarmush, M. L.; Berthiaume, F. Elastin-like Polypeptides: A Strategic Fusion Partner for Biologics. *Biotechnol. Bioeng.* **2016**, *113* (8), 1617–1627. https://doi.org/10.1002/bit.25998.
(18) Hassouneh, W.; Christensen, T.; Chilkoti, A. Elastin-Like Polypeptides as a Purification Tag for Recombinant Proteins. *Curr. Protoc. Protein Sci.* **2010**, *61* (1), 6.11.1-6.11.16. https://doi.org/10.1002/0471140864.ps0611s61.
(19) Bellucci, J. J.; Amiram, M.; Bhattacharyya, J.; McCafferty, D.; Chilkoti, A. Three-in-One Chromatography-Free Purification, Tag Removal, and Site-Specific Modification of Recombinant Fusion Proteins Using Sortase A and Elastin-like Polypeptides. *Angew. Chem. Int. Ed.* **2013**, *52* (13), 3703–3708. https://doi.org/10.1002/anie.201208292.
(20) Reguera, J.; Fahmi, A.; Moriarty, P.; Girotti, A.; Rodríguez-Cabello, J. C. Nanopore Formation by Self-Assembly of the Model Genetically Engineered Elastin-like Polymer [(VPGVG)2(VPGEG)(VPGVG)2]15. *J. Am. Chem. Soc.* **2004**, *126* (41), 13212–13213. https://doi.org/10.1021/ja047417f.
(21) Lampe, K. J.; Antaris, A. L.; Heilshorn, S. C. Design of Three-Dimensional Engineered Protein Hydrogels for Tailored Control of Neurite Growth. *Acta Biomater.* **2013**, *9* (3), 5590–5599. https://doi.org/10.1016/j.actbio.2012.10.033.
(22) Prieto, S.; Shkilnyy, A.; Rumplasch, C.; Ribeiro, A.; Arias, F. J.; Rodríguez-Cabello, J. C.; Taubert, A. Biomimetic Calcium Phosphate Mineralization with Multifunctional Elastin-Like Recombinamers. *Biomacromolecules* **2011**, *12* (5), 1480–1486. https://doi.org/10.1021/bm200287c.
(23) Olsen, B. D.; Kornfield, J. A.; Tirrell, D. A. Yielding Behavior in Injectable Hydrogels from Telechelic Proteins. *Macromolecules* **2010**, *43* (21), 9094–9099. https://doi.org/10.1021/ma101434a.
(24) Girotti, A.; Reguera, J.; Rodríguez-Cabello, J. C.; Arias, F. J.; Alonso, M.; Testera, A. M. Design and Bioproduction of a Recombinant Multi(Bio)Functional Elastin-like Protein Polymer Containing Cell Adhesion Sequences for Tissue Engineering Purposes. *J. Mater. Sci. Mater. Med.* **2004**, *15* (4), 479–484. https://doi.org/10.1023/B:JMSM.0000021124.58688.7a.

(25) Katyal, P.; Hettinghouse, A.; Meleties, M.; Hasan, S.; Chen, C.; Cui, M.; Sun, G.; Menon, R.; Lin, B.; Regatte, R.; Montclare, J. K.; Liu, C. Injectable Recombinant Block Polymer Gel for Sustained Delivery of Therapeutic Protein in Post Traumatic Osteoarthritis. *Biomaterials* **2022**, *281*, 121370. https://doi.org/10.1016/j.biomaterials.2022.121370.
(26) Hill, L. K.; Frezzo, J. A.; Katyal, P.; Hoang, D. M.; Ben Youss Gironda, Z.; Xu, C.; Xie, X.; Delgado-Fukushima, E.; Wadghiri, Y. Z.; Montclare, J. K. Protein-Engineered Nanoscale Micelles for Dynamic 19F Magnetic Resonance and Therapeutic Drug Delivery. *ACS Nano* **2019**, *13* (3), 2969–2985. https://doi.org/10.1021/acsnano.8b07481.
(27) Bhattacharyya, J.; Bellucci, J. J.; Weitzhandler, I.; McDaniel, J. R.; Spasojevic, I.; Li, X.; Lin, C.-C.; Chi, J.-T. A.; Chilkoti, A. A Paclitaxel-Loaded Recombinant Polypeptide Nanoparticle Outperforms Abraxane in Multiple Murine Cancer Models. *Nat. Commun.* **2015**, *6* (1), 7939. https://doi.org/10.1038/ncomms8939.
(28) Price, R.; Poursaid, A.; Ghandehari, H. Controlled Release from Recombinant Polymers. *J. Controlled Release* **2014**, *190*, 304–313. https://doi.org/10.1016/j.jconrel.2014.06.016.
(29) MacEwan, S. R.; Chilkoti, A. Applications of Elastin-like Polypeptides in Drug Delivery. *J. Controlled Release* **2014**, *190*, 314–330. https://doi.org/10.1016/j.jconrel.2014.06.028.
(30) Dautel, D. R.; Champion, J. A. Protein Vesicles Self-Assembled from Functional Globular Proteins with Different Charge and Size. *Biomacromolecules* **2021**, *22* (1), 116–125. https://doi.org/10.1021/acs.biomac.0c00671.
(31) Schreiber, A.; Huber, M. C.; Schiller, S. M. Prebiotic Protocell Model Based on Dynamic Protein Membranes Accommodating Anabolic Reactions. *Langmuir* **2019**, *35* (29), 9593–9610. https://doi.org/10.1021/acs.langmuir.9b00445.
(32) Park, W. M.; Champion, J. A. Thermally Triggered Self-Assembly of Folded Proteins into Vesicles. *J. Am. Chem. Soc.* **2014**, *136* (52), 17906–17909. https://doi.org/10.1021/ja5090157.
(33) Huber, M. C.; Schreiber, A.; von Olshausen, P.; Varga, B. R.; Kretz, O.; Joch, B.; Barnert, S.; Schubert, R.; Eimer, S.; Kele, P.; Schiller, S. M. Designer Amphiphilic Proteins as Building Blocks for the Intracellular Formation of Organelle-like Compartments. *Nat. Mater.* **2015**, *14* (1), 125–132. https://doi.org/10.1038/nmat4118.
(34) Fluegel, S.; Buehler, J.; Fischer, K.; McDaniel, J. R.; Chilkoti, A.; Schmidt, M. Self-Assembly of Monodisperse Oligonucleotide-Elastin Block Copolymers into Stars and Compound Micelles. *Chem. - Eur. J.* **2011**, *17* (20), 5503–5506. https://doi.org/10.1002/chem.201100436.
(35) Wang, B.; Pan, R.; Zhu, W.; Xu, Y.; Tian, Y.; Endo, M.; Sugiyama, H.; Yang, Y.; Qian, X. Short Intrinsically Disordered Polypeptide–Oligonucleotide Conjugates for Programmed Self-Assembly of Nanospheres with Temperature-Dependent Size Controllability. *Soft Matter* **2021**, *17* (5), 1184–1188. https://doi.org/10.1039/D0SM01817A.
(36) Wang, B.; Fang, H.; Zhu, W.; Xu, Y.; Yang, Y.; Qian, X. Dynamic Compartmentalization of Peptide–Oligonucleotide Conjugates with Reversible Nanovesicle–Microdroplet Phase Transition Behaviors. *ACS Appl. Mater. Interfaces* **2022**, *14* (32), 36998–37008. https://doi.org/10.1021/acsami.2c05268.
(37) Molla, M. R.; Prasad, P.; Thayumanavan, S. Protein-Induced Supramolecular Disassembly of Amphiphilic Polypeptide Nanoassemblies. *J. Am. Chem. Soc.* **2015**, *137* (23), 7286–7289. https://doi.org/10.1021/jacs.5b04285.
(38) Azagarsamy, M. A.; Yesilyurt, V.; Thayumanavan, S. Disassembly of Dendritic Micellar Containers Due to Protein Binding. *J. Am. Chem. Soc.* **2010**, *132* (13), 4550–4551. https://doi.org/10.1021/ja100746d.
(39) Wang, H.; Zhuang, J.; Raghupathi, K. R.; Thayumanavan, S. A Supramolecular Dissociation Strategy for Protein Sensing. *Chem. Commun.* **2015**, *51* (97), 17265–17268. https://doi.org/10.1039/C5CC07408H.
(40) Yoshii, T.; Mizusawa, K.; Takaoka, Y.; Hamachi, I. Intracellular Protein-Responsive Supramolecules: Protein Sensing and In-Cell Construction of Inhibitor Assay System. *J. Am. Chem. Soc.* **2014**, *136* (47), 16635–16642. https://doi.org/10.1021/ja508955y.

(41) Dai, M.; Georgilis, E.; Goudounet, G.; Garbay, B.; Pille, J.; van Hest, J. C. M.; Schultze, X.; Garanger, E.; Lecommandoux, S. Refining the Design of Diblock Elastin-Like Polypeptides for Self-Assembly into Nanoparticles. *Polymers* **2021**, *13* (9), 1470. https://doi.org/10.3390/polym13091470.
(42) Grazon, C.; Baer, R. C.; Kuzmanović, U.; Nguyen, T.; Chen, M.; Zamani, M.; Chern, M.; Aquino, P.; Zhang, X.; Lecommandoux, S.; Fan, A.; Cabodi, M.; Klapperich, C.; Grinstaff, M. W.; Dennis, A. M.; Galagan, J. E. A Progesterone Biosensor Derived from Microbial Screening. *Nat. Commun.* **2020**, *11* (1), 1276. https://doi.org/10.1038/s41467-020-14942-5.
(43) Grazon, C.; Chern, M.; Lally, P.; Baer, R. C.; Fan, A.; Lecommandoux, S.; Klapperich, C.; Dennis, A. M.; Galagan, J. E.; Grinstaff, M. W. The Quantum Dot *vs.* Organic Dye Conundrum for Ratiometric FRET-Based Biosensors: Which One Would You Chose? *Chem. Sci.* **2022**, *13* (22), 6715–6731. https://doi.org/10.1039/D1SC06921G.
(44) Tornøe, C. W.; Christensen, C.; Meldal, M. Peptidotriazoles on Solid Phase: [1,2,3]-Triazoles by Regiospecific Copper(I)-Catalyzed 1,3-Dipolar Cycloadditions of Terminal Alkynes to Azides. *J. Org. Chem.* **2002**, *67* (9), 3057–3064. https://doi.org/10.1021/jo011148j.
(45) Rostovtsev, V. V.; Green, L. G.; Fokin, V. V.; Sharpless, K. B. A Stepwise Huisgen Cycloaddition Process: Copper(I)-Catalyzed Regioselective "Ligation" of Azides and Terminal Alkynes. *Angew. Chem. Int. Ed.* **2002**, *41* (14), 2596–2599. https://doi.org/10.1002/1521-3773(20020715)41:14<2596::AID-ANIE2596>3.0.CO;2-4.
(46) Gutsmiedl, K.; Fazio, D.; Carell, T. High-Density DNA Functionalization by a Combination of Cu-Catalyzed and Cu-Free Click Chemistry. *Chem. – Eur. J.* **2010**, *16* (23), 6877–6883. https://doi.org/10.1002/chem.201000363.
(47) Jewett, J. C.; Bertozzi, C. R. Cu-Free Click Cycloaddition Reactions in Chemical Biology. *Chem. Soc. Rev.* **2010**, *39* (4), 1272–1279. https://doi.org/10.1039/B901970G.
(48) Vieregg, J. R.; Lueckheide, M.; Marciel, A. B.; Leon, L.; Bologna, A. J.; Rivera, J. R.; Tirrell, M. V. Oligonucleotide–Peptide Complexes: Phase Control by Hybridization. *J. Am. Chem. Soc.* **2018**, *140* (5), 1632–1638. https://doi.org/10.1021/jacs.7b03567.
(49) Shah, S.; Leon, L. Structural Dynamics, Phase Behavior, and Applications of Polyelectrolyte Complex Micelles. *Curr. Opin. Colloid Interface Sci.* **2021**, *53*, 101424. https://doi.org/10.1016/j.cocis.2021.101424.

Table of Contents graphic

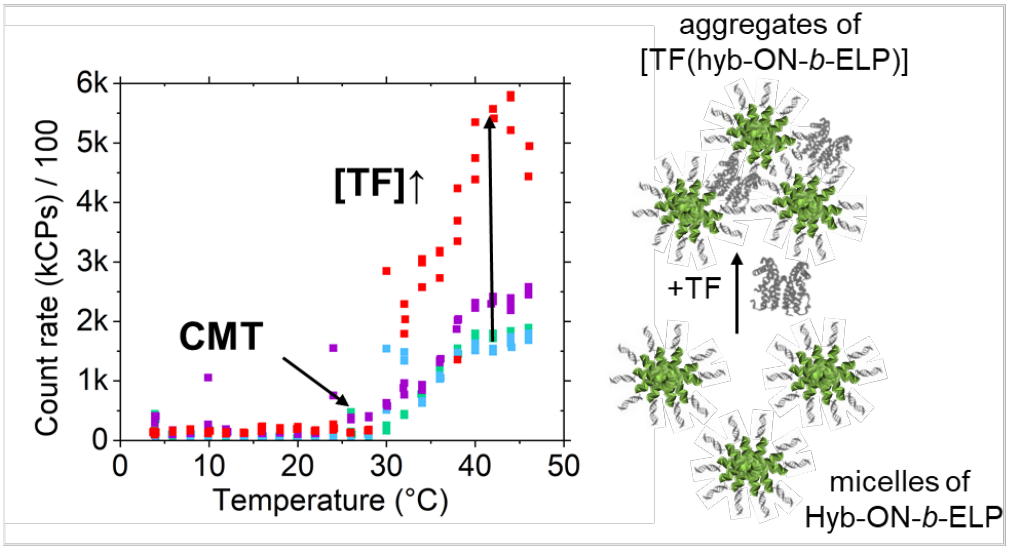

Transcription-factor-induced aggregation of biomimetic oligonucleotide-*b*-protein micelles

Chloé Grazon,[1,2,3] Elisabeth Garanger,[2] Pierre Lalanne,[2] Emmanuel Ibarboure,[2] James E. Galagan,[4] Mark W. Grinstaff,[3,5*] and Sébastien Lecommandoux[2*]

1 Univ. Bordeaux, CNRS, Bordeaux INP, ISM, UMR 5255, F-33400 Talence, France.

2 Univ. Bordeaux, CNRS, Bordeaux INP, LCPO, UMR 5629, F-33600, Pessac, France.

3 Department of Chemistry, Boston University, Boston, MA 02215, USA.

4 Department of Microbiology, Boston University, Boston, MA 02118, USA.

5 Department of Biomedical Engineering, Boston University, Boston, MA 02215, USA.

Keywords: DNA, elastin-like polypeptide, diblock bioconjugates, self-assembly, supramolecular, thermosensitivity

Table S1. Sequences of oligonucleotides used in this study

ON	Sequence	Bases	MW (g/mol)	Tm* (°C)
ON-NH_2	/5AmMC6/TTTT AAC TAG CCG TTC GGC TAG TT	24	7504	56.4
Bt-hybON	/5Biosg/AA CTA GCC GAA CGG CTA GTT	20	6519	56.2
hybON	/5/AA CTA GCC GAA CGG CTA GTT	20	6126	56.2

* Melting Points values are given by the ON supplier, and corresponds to theorical values in 50 mM NaCl.

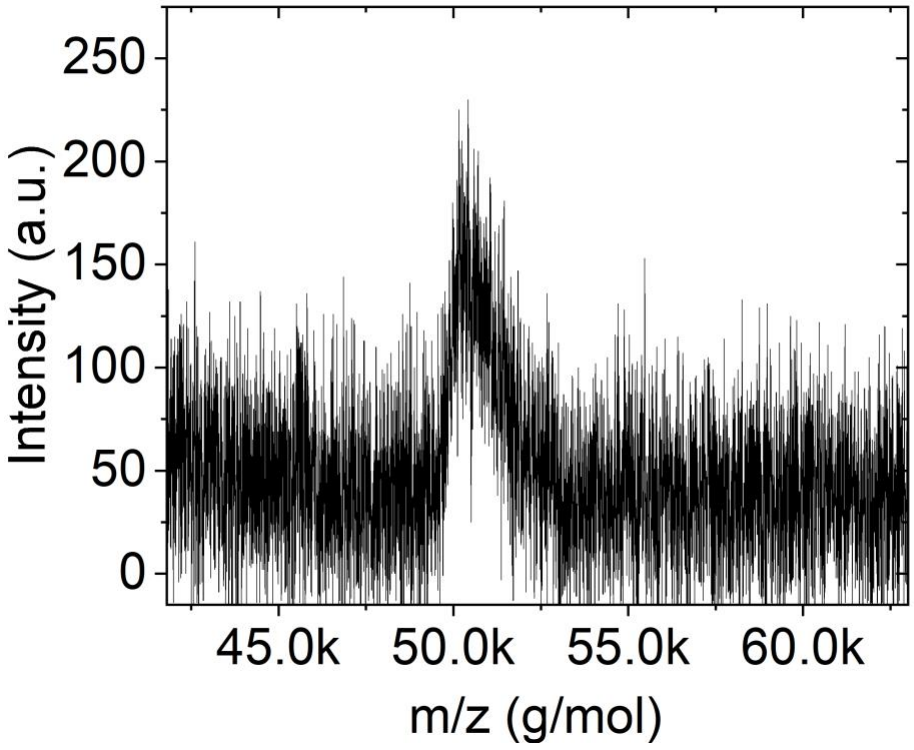

Figure S1 MALDI-TOF mass spectra of the ON-*b*-ELP (m/z~50,3 kg/mol)

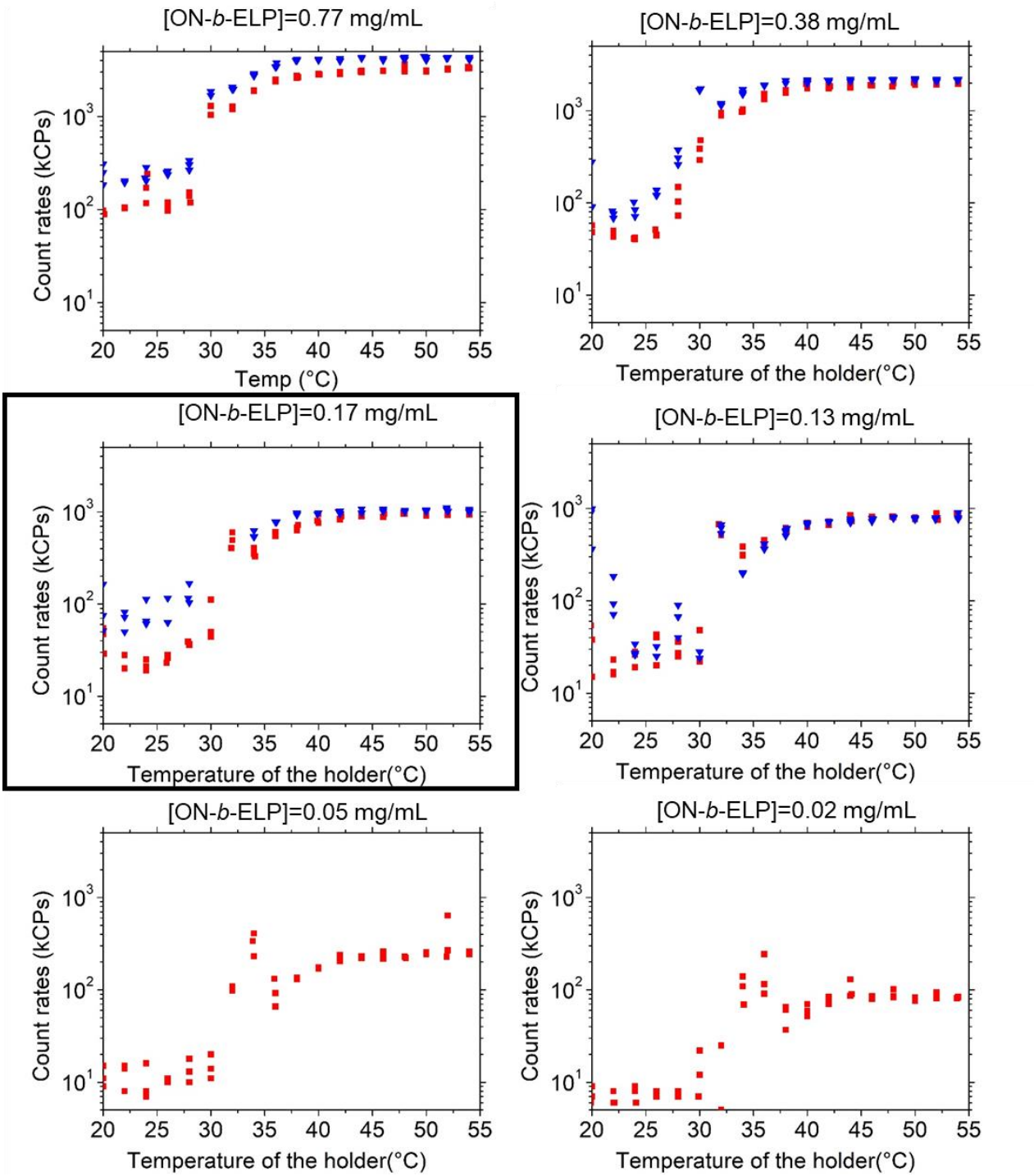

Figure S2. Scattered light intensity (count rates) of ON-*b*-ELP measured by DLS at different temperatures and concentrations in HBS (n=3). The red points correspond to a rise in temperature, while the blue points correspond to a fall. The data for the concentration used for the rest of the study (0.17 mg/mL) are highlighted with a black frame.

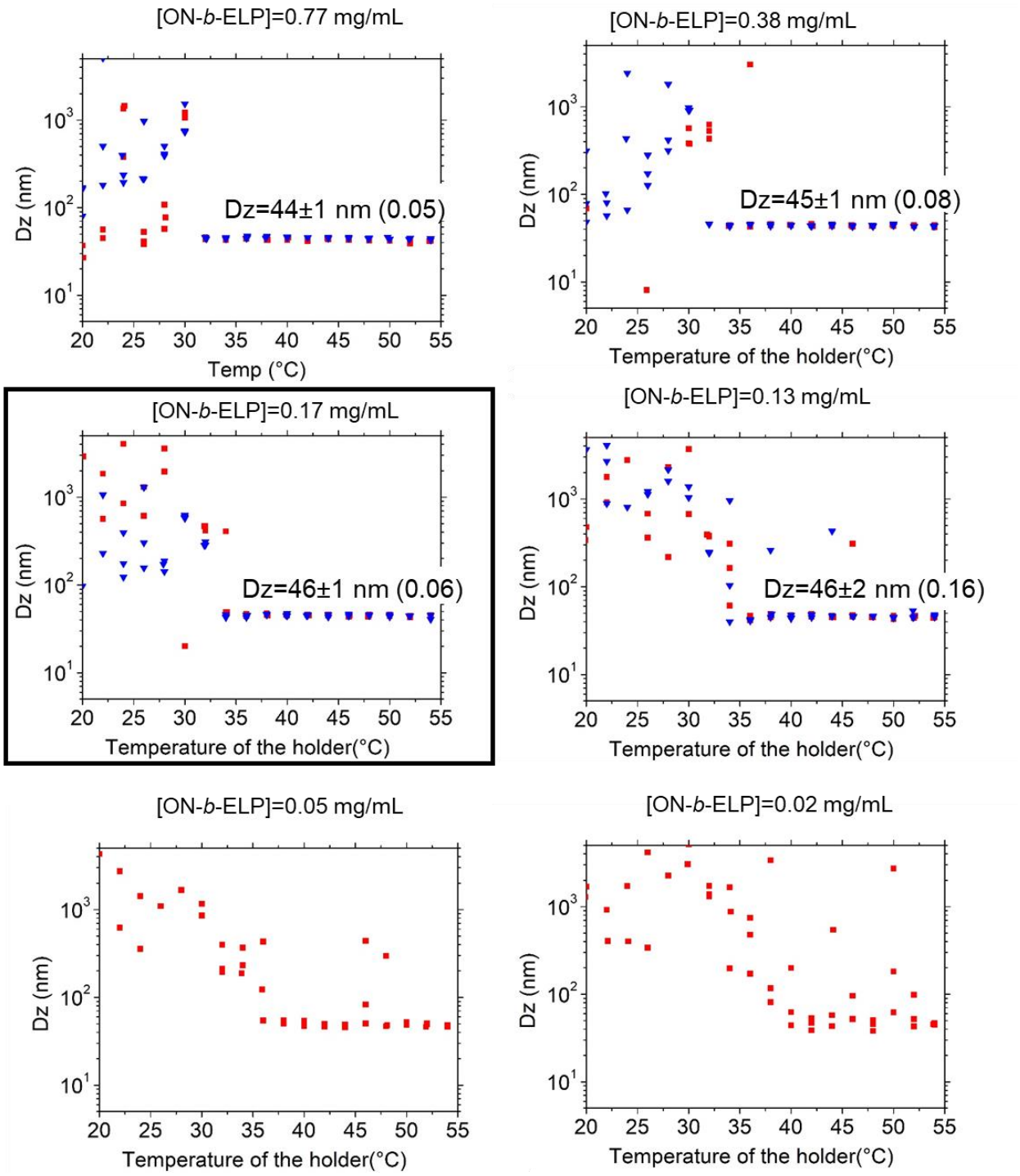

Figure S3. Z-averaged hydrodynamic diameters of ON-*b*-ELP measured by DLS at different temperatures and concentrations in HBS (n=3). As an indication, averaged D_z (± standard deviation on n=6) and dispersity indexes in brackets are indicated on the curves, above the CMT. The red points correspond to a rise in temperature, while the blue points correspond to a fall. The data for the concentration used for the rest of the study (0.17 mg/mL) are highlighted with a black frame.

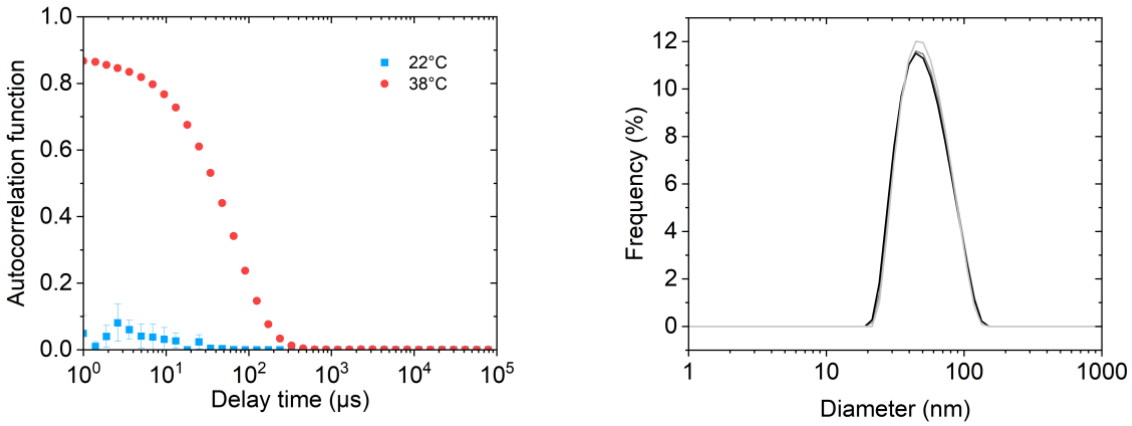

Figure S4. Left: Auto-correlation profiles of the ON-*b*-ELP (0.17 mg/mL, 3.4 μM) at 22°c or 38°C in HBS. Error bar on n=3. Right: Size distribution of the ON-*b*-ELP (0.17 mg/mL, 3.4 μM) micelles at 38°C, D_z = 46±1 nm (dispersity < 0.1).

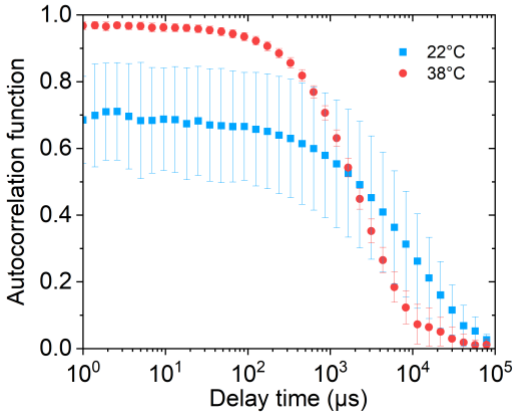

Figure S5. Auto-correlation profiles of the ELP (0.13 mg/mL, 3.1 μM) at 22°c or 38°C in HBS. Error bar on n=3.

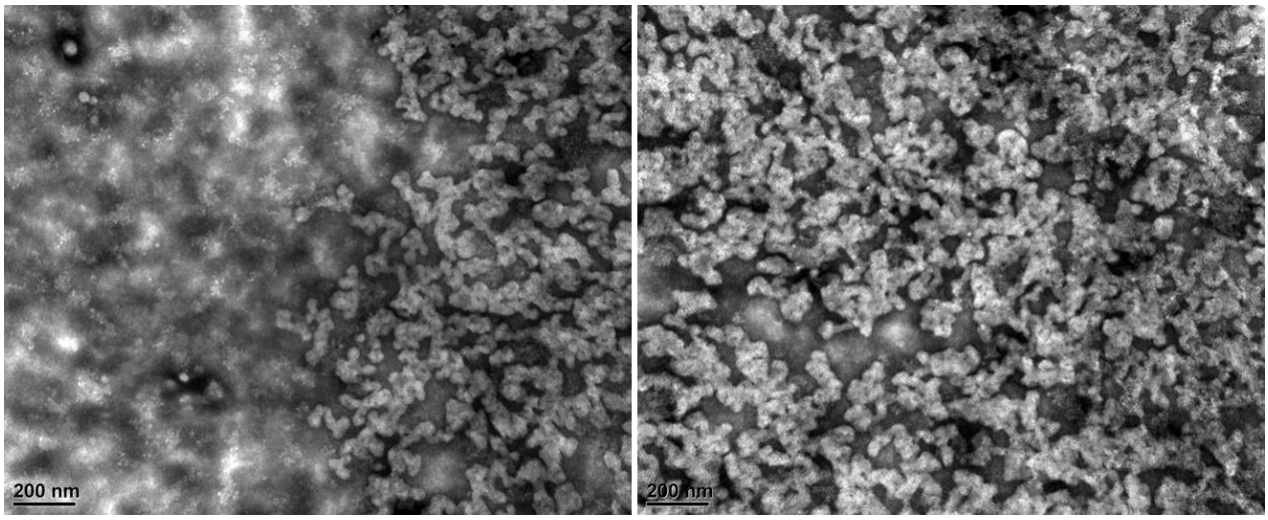

Figure S6 Transmission Electron Microscopy images of ON-*b*-ELP deposited on a copper grid at 37°C and stained with uranyl acetate.

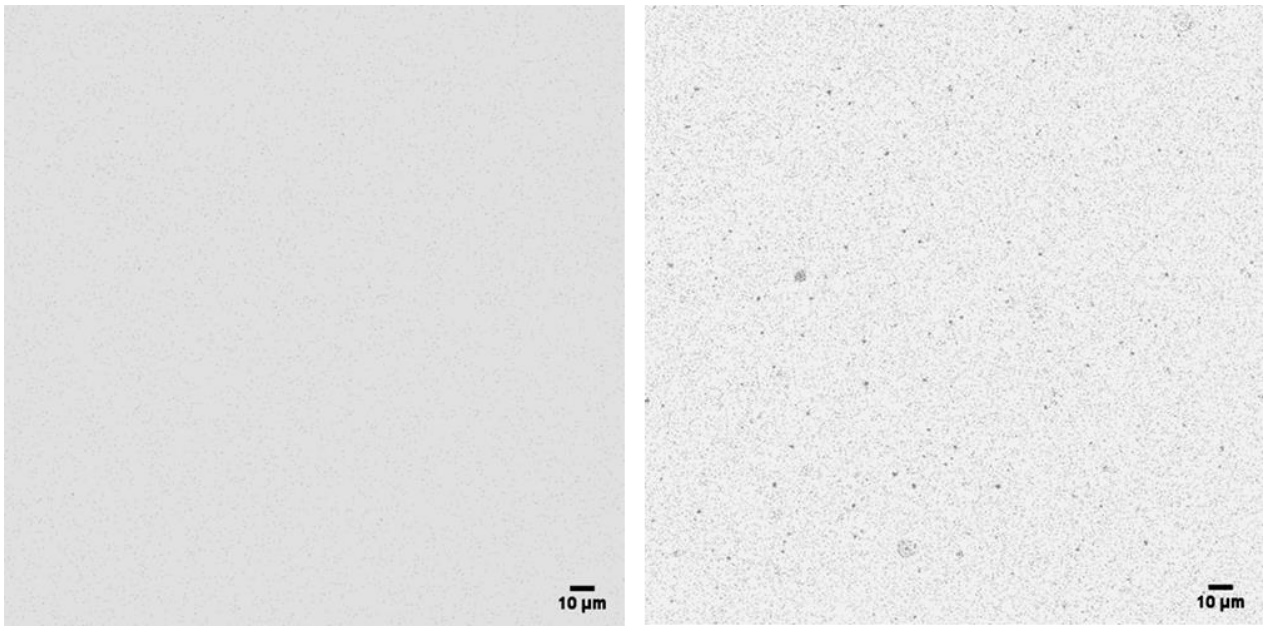

Figure S7. Confocal microscope images of ON-*b*-ELP at 3.4 µM, labelled with Nile Red, below (left) and above (right, T=40°C) the CMT in HBS. Colors are inverted so that the black points represent the fluorescent species with a dark (white) background.

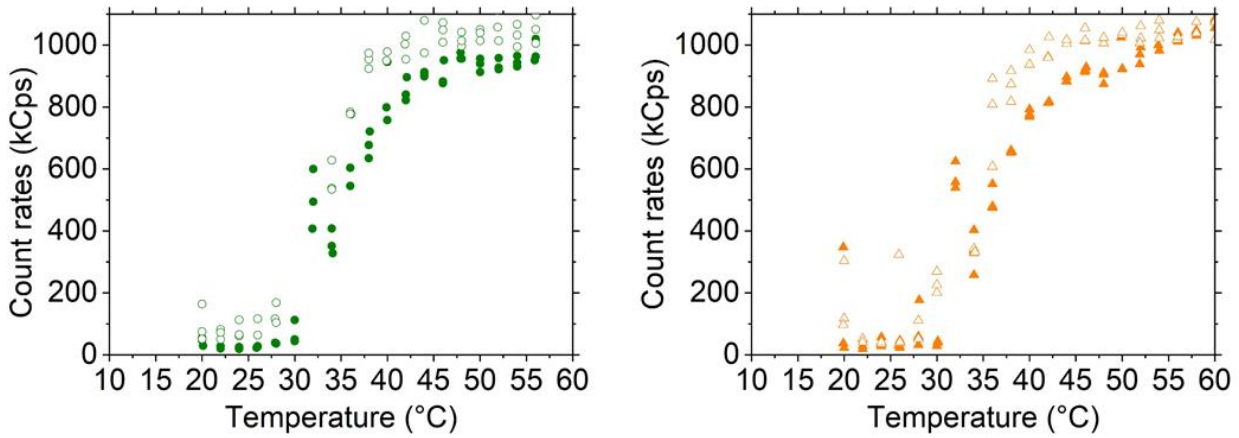

Figure S8. Scattering intensity (count rates) measured by DLS of ON-*b*-ELP (left) and bt-hyb-ON-*b*-ELP for a heating (plain symbols) and cooling (empty symbols) ramps in HBS. Diblocks are analyzed at 0.17 mg/mL, *i.e.*, 3.4 µM.

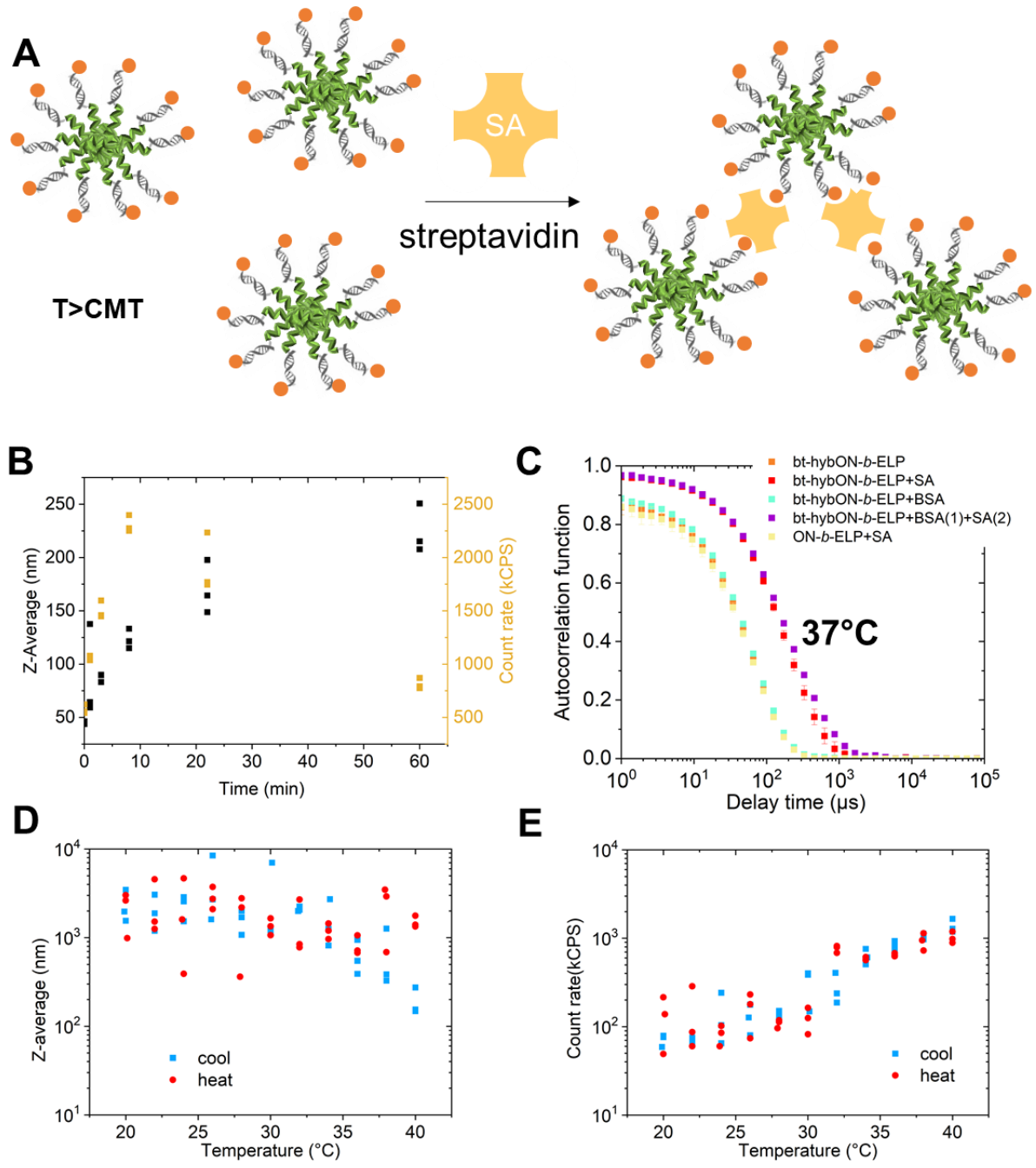

Figure S9 A. Illustration of bt-hyb-ON-*b*-ELP micelles aggregation by addition of streptavidin (SA). B. After addition of SA (4 μM) to bt-hyb-ON-*b*-ELP (3.4 μM), following of the aggregates formation over 60 min at 37±1°C in HBS.C. Auto-correlation profiles of the micelles (0.17 mg/mL, 3.4 μM) at 37±1°C in HBS in different conditions (SA and/or BSA proteins are added to a final concentration of 4 μM each). D and E temperature slopes on bt-hyb-ON-*b*-ELP after SA addition at 37±1°C in HBS.

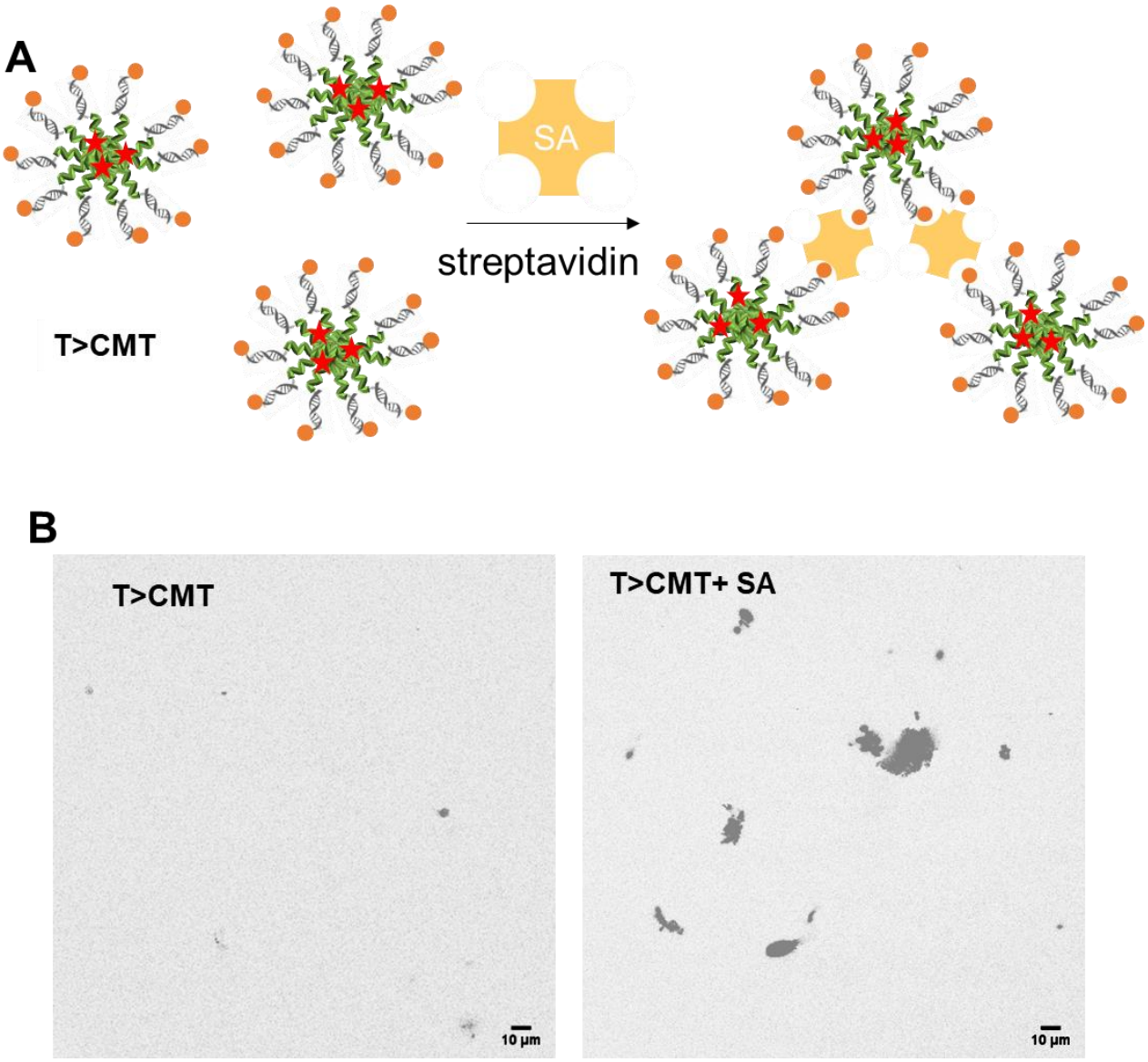

Figure S10 A. Bt-hyb-ON-*b*-ELP micelles are labelled with the Nile Red lipophilic probe Addition of streptavidin to bt-hyb-ON-*b*-ELP implies aggregation of the micelles. B. Confocal microscopy above the CMT (T=40°C). Left: micelles of bt-hyb-ON-*b*-ELP at 3.4 µM. Right: Addition of SA (10 µM) to the sample and observation of bigger aggregates. Colors are inverted so that the black points represent the fluorescent species with a dark (white) background.

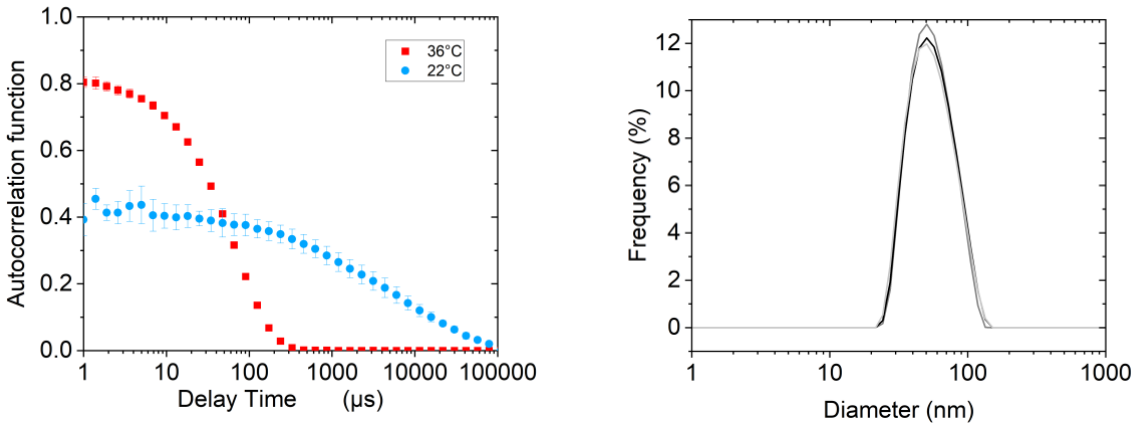

Figure S11. Left: Auto-correlation profiles of the hyb-ON-*b*-ELP (0.17 mg/mL, 3.4 µM) at 22°c or 36°C in HBS. Error bar on n=3. Right: Size distribution of the hyb-ON-*b*-ELP (0.17 mg/mL, 3.4 µM) micelles at 36°C, D_z = 49±2 nm (dispersity = 0.15).

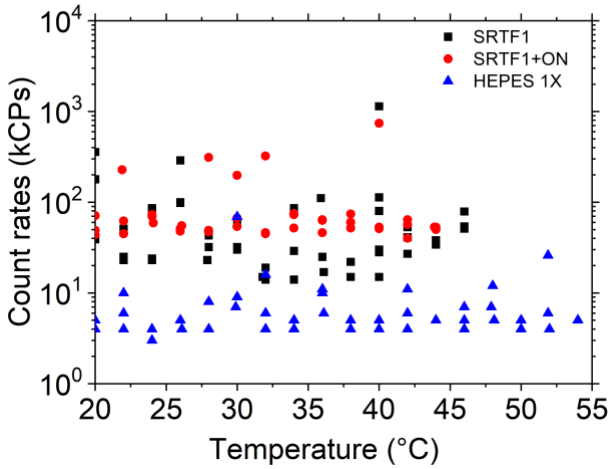

Figure S12 Light scattering intensity of solutions without ELP: SRTF1 at 10 µM, SRTF1+ON-NH_2 at 10 µM, HBS.